Oil & Gas Science and Technology – Rev. IFP Energies nouvelles, Vol. 69 (2014), No. 7, pp. 1251-1267

DOI: 10.2516/ogst/2013208

Blowout in Gas Storage Caverns

H. Djizanne[1]*, P. Bérest[1], B. Brouard[2] and A. Frangi[3]

[1] *LMS, École Polytechnique ParisTech, École des Mines de Paris, École des Ponts et Chaussées, UMR 7649 CNRS, route de Saclay, 91120 Palaiseau - France*
[2] *Brouard Consulting, 101 rue du temple, 75003 Paris - France*
[3] *Politecnico di Milano, Piazza Leonardo da Vinci, 32, 20133 Milano - Italy*
e-mail: djakeun@lms.polytechnique.fr - berest@lms.polytechnique.fr - contact@brouard-consulting.com - attilio.frangi@polimi.it

* Corresponding author

Abstract — *A small number of blowouts from gas storage caverns has been described in the literature. Gas flow lasted several days before the caverns were emptied. In this paper, we suggest simplified methods that allow for computing blowout duration, and evolution of gas temperature and pressure in the cavern and in the well. This method is used to compute air flow from an abandoned mine, an accident described by Van Sambeek in 2009, and a natural gas blowout in an underground storage facility in Kansas. The case of a hydrogen storage cavern also is considered, as it is known that hydrogen depressurization can lead, in certain cases, to an increase in hydrogen temperature.*

Résumé — **Éruption en cavités de stockage de gaz** — Un petit nombre d'éruptions en cavités salines de stockage de gaz a été décrit dans la littérature. L'écoulement de gaz dure plusieurs jours avant que les cavités ne se vident complètement. Dans cet article, nous proposons une méthode de calcul de la durée de l'éruption et de l'évolution des paramètres majeurs du système tels que la température, la pression et la vitesse du gaz dans la cavité ou dans le puits. Cette méthode est utilisée pour calculer le débit d'air expulsé par un puits d'accès à une mine de sel abandonnée, un accident décrit par Van Sambeek en 2009, et une éruption suivie d'une combustion du gaz naturel sur un site de stockage souterrain de gaz naturel au Kansas. Le cas d'une cavité de stockage d'hydrogène est également examiné, avec le souci de vérifier si la détente de l'hydrogène peut conduire, dans certains cas, à une augmentation de sa température.

LIST OF SYMBOLS

a	van der Waals gas coefficient, measures attraction between particles, J.m^3/kg^2
b	van der Waals gas coefficient, excluded volume per unit of mass of a gas, m^3/kg
C_p	Heat capacity at constant pressure, J/kg.K
C_v	Heat capacity at constant volume, J/kg.K
D	Well diameter, m
e	Internal energy, J
F	Friction coefficient, /m
f	Friction factor
g	Gravity acceleration, m/s^2
H	Borehole length, m
h	Gas enthalpy, J/kg
K	Thermal conductivity of salt, W/m.°C
k	Thermal diffusivity of salt, m^2/s
M	Molar mass, g/mol
m	Gas mass, kg
P	Pressure, Pa
P_{atm}	Atmospheric pressure, Pa
P_c	Cavern pressure, Pa
P_{wh}	Wellhead cavern pressure, Pa
Q	Heat flux at cavern wall, W
S	Gas entropy, J/K
t	Time, s
T	Temperature, K
T_c	Cavern temperature, K
T_{cr}	Critical temperature, K
T_{wh}	Wellhead gas temperature, K
u_c	Gas velocity at casing-shoe depth, m/s
u_{wh}	Wellhead gas velocity, m/s
V_0	Cavern volume, m^3
z	Depth, m

GREEK LETTERS

γ	Ratio of specific heats, $\gamma = C_p/C_v$
ε	Absolute roughness of the well, m
η	Kinematic viscosity of gas, m^2/s
$\dot{\mu}$	Mass flow, kg/s.m^2
v	Specific volume of gas, m^3/kg
v_c	Specific volume of cavern gas, m^3/kg
v_{wh}	Specific volume of wellhead gas, m^3/kg
ρ	Gas density, kg/m^3
Σ	Cross-sectional area of well, m^2
Σ_c	Actual surface of cavern walls, m^2

INTRODUCTION

A blowout is the uncontrolled release of crude oil and/or natural gas from an oil or gas well after pressure control systems have failed. It often is a dramatic accident when it affects a conventional reservoir, as the amount of gas or oil that can be released can be huge; blowout duration can be several months long. Blowouts from storage caverns of liquid or liquefied hydrocarbons have a different character, as the amount of products immediately released after wellhead failure is relatively small (Bérest and Brouard, 2003). Several examples of blowouts in gas storage caverns have been described in the literature, such as that in an ethane storage at Fort Saskatchewan, Canada (Alberta Energy and Utilities Board, 2002) or in a natural gas storage at Moss Bluff, Texas (Rittenhour and Heath, 2012). There were no casualties in these instances, as the gas rapidly ignited, although the entire inventory was lost. A somewhat similar accident occurred in a "compressed air storage" (in fact, an abandoned salt mine) at Kanopolis, Kansas; a complete description can be found in Van Sambeek (2009).

The most striking difference between a blowout in a well tapped in an oil or gas reservoir and a blowout in a gas-cavern well is that the blowout in a gas-cavern well is completed within a couple of days, as the gas inventory in a cavern is much smaller than in a reservior. Another difference is that the modeling of the thermodynamic behavior of gas in the cavern is much simpler than in a permeable reservoir, allowing a complete computation of the blowout.

In this paper, a simple method for computing a blowout from a salt cavern is proposed. It involves relatively simple formulae and light numerical computations. Discussion of the numerical results focuses on blowout duration, gas rates at ground level and the evolutions of gas temperature in the cavern. This last issue is of special significance. The drop of gas temperature in a cavern during a blowout often is severe, and thermal tensile stresses are generated at the cavern wall (Bérest *et al.*, 2013). It has been suspected that these stresses lead to fracturing at the cavern wall, spalling and loss of cavern tightness, and correct assessment of cavern temperature is important in this context. In fact, it will be proved that low gas temperatures in the cavern are experienced during a relatively short period of time, and that the depth of penetration of temperature changes at cavern walls is too small to generate deep tensile fractures.

1 EVOLUTION OF GAS TEMPERATURE AND PRESSURE IN THE CAVERN

1.1 Salt Caverns

Salt caverns currently are used for storing hydrocarbons, air or hydrogen. These caverns are created through solution mining. In this system, a well is drilled to the salt formation, and cased and cemented to the formation. A smaller tube is set inside the casing, as a straw in a bottle. Soft water is injected through the central tube. The water leaches out the salt, and the formed brine is withdrawn from the cavern through the annular space between the central string and the casing. After a year or so, a large cavern is created. Its depth ranges from 200 m to 2 000 m, and its volume ranges from 10 000 m^3 to several millions m^3. When solution mining is completed, the cavern is filled with saturated brine. Gas then is injected through the annular space, and brine is withdrawn through the central tubing ("debrining"). A small amount of brine is left at the cavern bottom, and the gas in the cavern is wet. A typical operation cycle includes withdrawal during winter and injection during summer. Minimum and maximum gas pressures typically range from, respectively, 15% to 90% of the geostatic pressure (*i.e.*, the weight of the overburden).

1.2 Energy Balance

Gas temperature, $T_c(t)$, and gas pressure, $P_c(t)$, can be considered almost uniform throughout the entire volume of a cavern (Bérest *et al.*, 2012). The stored gas is characterized by its state equation, which defines gas pressure (P) as a function of gas specific volume ($v = 1/\rho, \rho$ is the gas density) and of gas (absolute) temperature (T); by a thermodynamic potential, for instance, its enthalpy per unit of mass (h) or its internal energy per unit of mass ($e = h - Pv$):

$$P = P(v, T) \tag{1}$$

$$h = h(T, P) \tag{2}$$

The kinetic energy of gas in the cavern is neglected. The energy balance equation can be written:

$$m(\dot{e}_c + P_c\dot{v}_c) = Q + < \dot{m} > \left(h_{inj} - h_c\right) + L\dot{C} \tag{3}$$

where m is the mass of gas in the cavern, e_c is the gas internal energy, and:

$$\dot{e}_c + P_c\dot{v}_c = C_v\dot{T}_c + T_c(\partial P/\partial T)|_{v_c}\dot{v}_c$$

$< \dot{m} >= \dot{m}$ when $\dot{m} > 0$ and $< \dot{m} >= 0$ when $\dot{m} < 0$. When gas is injected in the cavern ($< \dot{m} >= \dot{m} > 0$), the difference between the enthalpy of the injected gas $\left(h_{inj}\right)$and the enthalpy of the cavern gas (h_c) must be taken into account. C is the amount of water vapor in the cavern, and L is the phase-change heat of water (from liquid phase to vapor phase). Q is the heat flux transferred from the rock mass to the cavern gas through the cavern wall, or:

$$Q = \int -K_{salt}\frac{\partial T_{salt}}{\partial n}da \tag{4}$$

where K_{salt} is the thermal conductivity of salt (typically, $K_{salt} = 6$ W/m.°C) and T_{salt} is the temperature of the rock mass.

1.3 Simplifications

In the following, it is assumed that the gas is ideal, $Pv = rT, e = C_vT$, and $\dot{e} + P\dot{v} = C_v\dot{T} + rT\dot{v}/v$. During a blowout, $\dot{m} < 0$ and $< \dot{m} >= 0$. During gas withdrawal, cavern volume, or V_0, experiences only a small change and can be considered constant, or $V_0 = mv$ and $m\dot{v} = -\dot{m}v$. Water vapor condenses during gas depressurization ("raining", or even "snowing", in the cavern); however, from the perspective of energy balance, this term is small and can be neglected.

The heat flux from the cavern is much more significant; it can be computed as follows. The evolution of temperature in the rock mass is governed by thermal conduction. Generally speaking, penetration of temperature changes in the rock mass is slow. For instance, when a cold gas temperature, T_0, has been kept constant over a t-long period of time on the (flat) surface of a half-space ($x > 0$) whose initial temperature (at $t = 0$) was T_∞, temperature evolution can be written:

$$T(x, t) = T_\infty + (T_0 - T_\infty)\mathrm{erfc}\left(\frac{x}{2\sqrt{kt}}\right)$$

where $k \approx 3 \times 10^{-6} m^2/s$ is the rock thermal diffusivity. Heat flux per unit area at the surface is:

$$Q = -K_{salt}(T_\infty - T_0)/\sqrt{\pi kt}$$

Rock temperature changes significantly (by more than: $(T - T_\infty)/(T_0 - T_\infty) = erfc(1/2) \simeq 50\%$) in a domain with a thickness of $d = \sqrt{kt}$, or $d \approx 1$ m after $t = 4$ days. Blowout in a gas cavern is a rapid process: it is completed within a week or less. During such a short period of time, temperature changes are not given time enough to penetrate deep into the rock mass and, from

the perspective of thermal conduction, cavern walls can be considered as a flat surface whose area equals the actual area of the cavern (in other words, for numerical computations, actual surface must be smoothed to eliminate shape irregularities whose radii of curvature are smaller than d), as was noted by Crotogino *et al.* (2001) and Krieter (2011).

When a varying temperature, $T_c = T_c(t)$, is applied on the surface, the heat flux per surface unit can be expressed as:

$$Q = \int_0^t -K_{salt} \frac{\dot{T}_c(\tau)}{\sqrt{\pi k(t-\tau)}} d\tau \tag{5}$$

When these simplifications are accepted, the heat balance equation can be written:

$$\frac{\dot{T}_c(t)}{v_c(t)} + (\gamma - 1)\frac{\dot{v}_c(t)T_c(t)}{v_c^2(t)} = -\frac{\Sigma_c K}{C_v V_0 \sqrt{k}} \int_0^t \frac{\dot{T}_c(\tau)}{\sqrt{\pi(t-\tau)}} d\tau \tag{6}$$

where Σ_c is the (actual) surface of the cavern walls. When the heat flux is neglected ($K = 0$), the thermodynamic behavior of gas is isentropic and $Tv^{\gamma-1}$ is constant as expected.

1.4 The case of a van der Waals Gas

In Section 6, the case of a hydrogen storage is discussed, in which a van der Waals equation — instead of an ideal gas equation — is more appropriate:

$$P = -a/v^2 + RT/(v-b)$$

and

$$h = C_v T - 2a/v + rTv/(v-b)$$

The heat balance equation can be written:

$$\frac{\dot{T}_c(t)}{v_c(t)} + (\gamma - 1)\frac{\dot{v}_c(t)T_c(t)}{v_c{}^2 - bv_c} = -\frac{\Sigma_c K}{C_v V_0 \sqrt{k}} \int_0^t \frac{\dot{T}_c(\tau)}{\sqrt{\pi(t-\tau)}} d\tau \tag{7}$$

1.5 An Example

Equation (6) was validated against the results of a withdrawal test performed in a gas-storage cavern at Melville (Canada), described by Crossley (1996). The measured flow rate, cavern pressure and temperature are drawn in Figure 1. The withdrawal period was 5 days long. The following values were selected: $\gamma = 1.305$, and $C_p = 2\,237$ J/kg.K. The cavern volume is $V_0 = 46\,000$ m^3. Cavern shape was unknown, and the surface of the cavern walls was selected to be twice the surface of a sphere whose volume equals the actual cavern volume. Note that slightly before the end of the withdrawal phase (day 5), gas starts warming, as the heat flux from the rock mass becomes quite high.

2 EVOLUTION OF GAS TEMPERATURE AND PRESSURE IN THE WELLBORE

In this section, the flow of gas through the well is discussed. Here, gas temperature, pressure or specific volume are functions of z ($z = 0$ at the cavern top or casing shoe and $z = H$ at the wellhead).

2.1 Main Assumptions

Duct

Duct diameter, D, is assumed to be constant all along the well; hence, the cross-sectional area of the duct, Σ, is constant as well.

Adiabatic Flow

Gas temperature decreases in the cavern and borehole. Casing steel, cement and rock at the vicinity of the well experience large temperature changes and thermal contraction. Conversely, the amount of heat transferred from the rock mass to the gas is not able to change gas temperature significantly, as the flow rate of gas is extremely fast. Heat transfer from the rock mass is neglected, and gas flow is considered adiabatic. This issue was discussed in Brouard Consulting and RESPEC (2013).

Turbulent Flow

Except maybe at the end of the blowout, gas flow is turbulent. The effects of friction are confined to a thin boundary layer at the steel casing wall. The average gas velocity is uniform through any cross-sectional area (except, of course, in the boundary layer).

Steady-State Flow

The gas rate in a borehole typically is a couple hundreds of meters per second (more, when hydrogen is considered). In other words, only a few seconds are needed for gas to travel from the cavern top to ground level. Such a short period of time is insufficient for

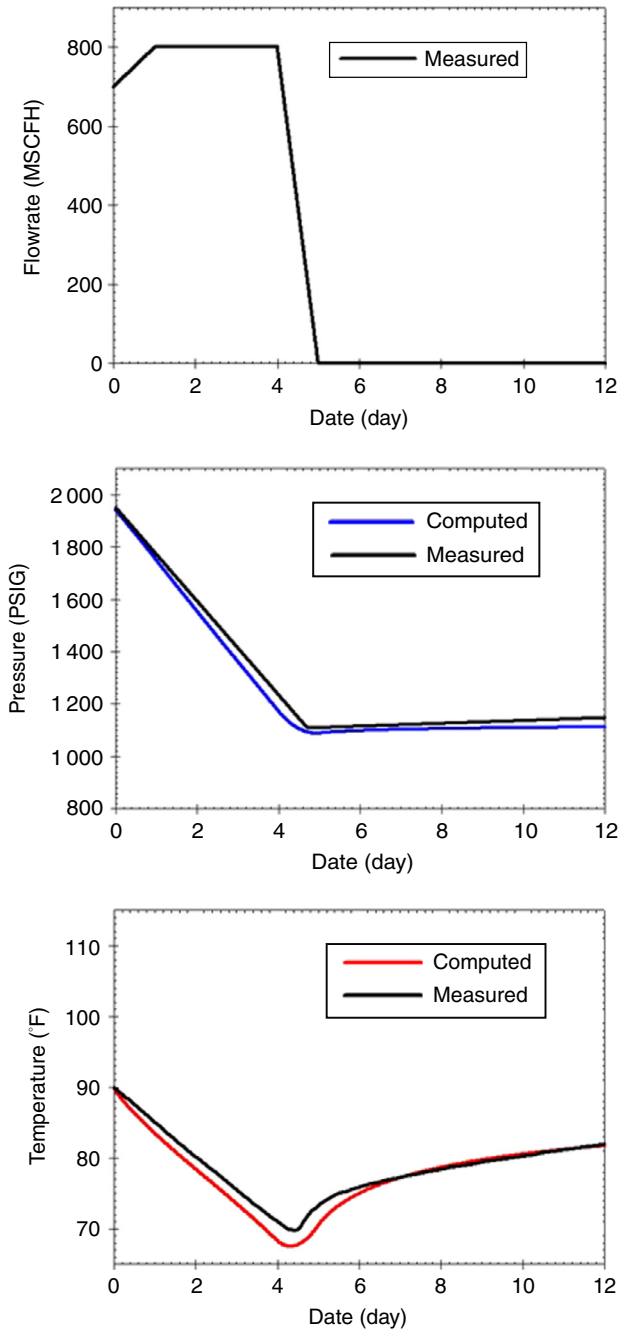

Figure 1

Melville Cavern: gas withdrawal rate, pressure and temperature evolutions, as observed (after Crossley, 1996) and computed.
1 MSCFH = 28 317 Nm^3/h, 1 MPa = 145 psig and 20°C = 68°F.

cavern pressure and temperature change significantly. Steady-state flow is assumed and, for simplicity, gas temperature, velocity etc. will be noted $T_c = T_c(z)$, $u = u(z)$, etc. (Obviously, when longer periods of time are considered, cavern pressure slowly decreases).

These assumptions, which are part of the so-called "Fanno-flow" model, are commonly accepted (Von Vogel and Marx, 1985), although Ma *et al.* (2011) consider an "isothermal" flow in the well.

2.2 Equations

In addition to Equations (1) and (2), gas flow can be described by the following set of equations:

$$\dot{\mu} = \frac{u(z)}{v(z)} = -\frac{V_0}{\Sigma}\frac{\dot{v}(z)}{v^2(z)} \tag{8}$$

$$\frac{dh}{dz} + u\frac{du}{dz} + g = 0 \tag{9}$$

$$v\frac{dP}{dz} + u\frac{du}{dz} + g = -f(u) \tag{10}$$

$$u\frac{dS}{dz} \geq 0 \tag{11}$$

Equation (8) is the mass conservation equation, where u and v define celerity and specific volume, respectively, and $\dot{\mu} = u(z)/v(z)$ is a constant in the well. Equation (9) is the energy equation, where g is the gravity acceleration. Equation (10) is the momentum equation. Head losses per unit of length are described by $f(u) > 0$, where $f = f(u; D, \varepsilon, ...)$ is a function of gas velocity, duct diameter, wall roughness, etc. Statement (11) is the condition of positivity of entropy (S) change, which plays an important role in the context of the Fanno-flow model.

2.3 Boundary Conditions and Subsonic Flow

Equations (8) to (10) allow computation of gas pressure and gas temperature in the borehole. Boundary conditions are needed. Pressure and temperature in the cavern [$P_c = P(z = 0)$ and $T_c = T(z = 0)$] are assumed known at any instant. Then, the specific volume of gas, or v_c, can be computed through the state equation $P_c = P(v_c, T_c)$. In principle, gas pressure at the wellhead, P_{wh}, should be atmospheric: $P_{wh} = P_{atm}$.

However, this boundary condition cannot always be satisfied. It is known from thermodynamics textbooks that $dh(S, P) = TdS + vdP$; hence:

$$dh(S, v) = TdS - c^2 dv/v$$

where c is the velocity of sound. (For an ideal gas, $c^2 = \gamma Pv$.) When gravity is disregarded in a Fanno flow, $dh + udu = 0$, and $TdS = (c^2 - u^2)dv/v$. However, the sign of dS must not change; in other words, when the flow of gas is subsonic ($u_c < c_c$) at cavern top ($z = 0$), it must remain subsonic [$u(z) < c(z)$] in the borehole (except perhaps at ground level, $z = H$).

When applying the boundary condition, $P_{wh} = P_{atm}$, leads to a solution such that gas flow is supersonic in a part of the well (this may occur when cavern pressure is sufficiently high), another solution must be selected (Landau and Lifchitz, 1971, Section 91). This solution is constructed such that $u_{wh} = c_{wh}$. (The flow, which is sonic at ground level, is said to be "choked".) In such a case, no constraint is applied to P_{wh}, which, in general, is larger than atmospheric. Conversely, when the cavern pressure is relatively small, the gas flow is said to be "normal". Even at ground level, the gas rate is significantly slower than the speed of sound, and the boundary condition $P_{wh} = P_{atm}$ applies.

2.4 Simplifications

The following simplified version of this set of equations allows a closed-form solution to be obtained.

Body Forces

Body forces are disregarded, $g = 0$. (However, the case when $g \neq 0$ is discussed in Appendix A; it has been proven that, in practical terms, this case does not lead to significant differences.)

Colebrook's Equation

Our main interest is in gas average velocities larger than $u = 1\,\text{m/s}$ (and up to several hundreds of m/s). Typically, air viscosity is $\eta = 1.3 \times 10^{-5}\ \text{m}^2/\text{s}$, duct diameter is $D = 0.2\,\text{m}$, and Reynolds number ($\text{Re} = uD/\eta$) is larger than 10^4. In this context, head losses can be written $f(u) = Fu^2$, where $F = f/2D$ is the friction coefficient, and f is the friction factor. Especially at the beginning of a blowout, when the velocity of gas is high and the Reynolds number is very large, the Colebrook's equation is written:

$$\frac{1}{\sqrt{f}} = -2\log_{10}\left(\frac{\varepsilon}{3.71D}\right) \tag{12}$$

where ε is the well roughness. ($\varepsilon = 0.02\,\text{mm}$ is a typical value.)

Gas State Equation

The gas state equation, $P = P(v, T)$, can be simplified as in the following two cases. In the first case, the gas (typically, natural gas or air) is ideal — *i.e.*, its state equation is:

$$Pv = rT, r = C_p - C_v, \gamma = C_p/C_v$$

and its enthalpy can be written $h = C_pT$, where the heat capacity of the gas at constant pressure C_p is constant. In the second case, the gas (typically, hydrogen) is of the van der Waals type — *i.e.*, its state equation is:

$$P = -\text{a}/v^2 + RT/(v - b)$$

where a, b are two constants, and its enthalpy is:

$$h = C_vT - 2\text{a}/v + rTv/(v - b)$$

where the heat capacity of the gas at constant volume C_v is constant.

The properties of gases used in this paper are presented in Table 1 (from gas encyclopedia, *Air Liquide*, 2012; pressure and temperature are 10^5 Pa and 298.15 K respectively).

2.5 Model Assessment

The aim of this paper is to provide a clear picture of the main phenomena that affect gas flow during a blowout, although results are indicative rather than exact. In fact, the model suffers from the following three flaws:

- head losses are roughly estimated by the simplified Colebrook's equation; in fact, actual coefficient F is a function of the flow rate, especially when this rate is small;
- even the van der Waals state equation is a less than perfect description of the actual behavior of hydrogen, and heat capacity, C_v, is a function of temperature;
- at the end of a blowout, gas flow rates are low, and the simplifications considered in Section 2.4 no longer hold.

A more precise description of gas behavior can be taken into account in Equations (1) and (2) — for instance, $C_v = C_v(T, v)$ and $Pv = rTZ(T, P)$. However, when such a description is accepted, numerical computations are required to compute the flow of gas in the well.

3 AIR OR NATURAL-GAS FLOW

3.1 Momentum Equation

In this Section, Equations (8) to (11) are used to obtain a relation between gas temperature in the cavern, T_c, and the specific mass of the gas in the cavern, v_c. Taking into

TABLE 1
Gases constants

Gases	C_p (J/kg.K)	C_v (J/kg.K)	γ(-)	M (g/mol)	a (J.m^3/kg^2)	b (m^3/kg)
Air	1 010	719	1.402	28.95	–	–
CH_4	2 237	1 714	1.305	16.043	–	–
H_2	14 831	10 714	1.384	2.016	6 092	0.013

account the simplifications noted in Section 2.4, energy Equation (6) can be re-written as:

$$C_pT(z) + \dot{\mu}^2 v^2(z)/2 = C_pT_c + \dot{\mu}^2 v_c^2 2 \tag{13}$$

Or

$$P(z) = \left(P_c + \frac{\gamma-1}{2\gamma}\dot{\mu}^2 v_c\right)\frac{v_c}{v(z)} - \left(\frac{\gamma-1}{2\gamma}\right)\dot{\mu}^2 v(z) \tag{14}$$

and momentum Equation (10) can be written as:

$$\left(\frac{rT_c}{\dot{\mu}^2} + \frac{\gamma-1}{2\gamma}v_c^2\right)\frac{1}{v^3(z)} - \frac{\gamma+1}{2\gamma v(z)} = F\frac{dz}{dv}(z) \tag{15}$$

Note that this equation also can be written:

$$c^2(z) - u^2(z) = \gamma\dot{\mu}^2 v^3(z) F\frac{dz}{dv}(z)$$

Because only solutions resulting in $u^2 < c^2$ are considered, v is an increasing function of z.

Integration of momentum Equation (15) from $z = 0$ (casing shoe) to $z = H$ (wellhead) leads to:

$$\frac{1}{2}\left[\left(\frac{rT_c}{\dot{\mu}^2} + \frac{\gamma-1}{2\gamma}v_c^2\right)\left(\frac{1}{v_c^2} - \frac{1}{v_{wh}^2}\right)\right] - \left(\frac{\gamma+1}{4\gamma}\right)Log\frac{v_{wh}^2}{v_c^2} = FH \tag{16}$$

3.2 Normal Flow

Gas pressure at ground level is, in principle, atmospheric, $P_{wh} = P_{atm}$:

$$P_{wh} = \left(rT_c + \frac{\gamma-1}{2\gamma}\dot{\mu}^2 v_c^2\right)\frac{1}{v_{wh}} - \left(\frac{\gamma-1}{2\gamma}\right)\dot{\mu}^2 v_{wh} = P_{atm} \tag{17}$$

The positive solution of this second-degree equation (with respect to v_{wh}) can be computed easily, and its combination with Equation (8) leads to the following differential equation:

$$\dot{v}_c = -\Sigma_c v_c \dot{\mu}(rT_c, v_c, \gamma, FH, P_{atm})/V_0 \tag{18}$$

However, this solution is valid only when Equation (11) is true (normal flow) — *i.e.*, when:

$$c^2 - u^2 = \gamma Pv - \dot{\mu}^2 v^2 = \gamma\left(rT_c + \frac{\gamma-1}{2\gamma}\dot{\mu}^2 v_c^2\right) - \left(\frac{\gamma+1}{2}\right)\dot{\mu}^2 v^2 > 0 \tag{19}$$

3.3 Choked Flow

When condition (19) is not met, the solution (normal flow) must be rejected. The boundary condition $P_{wh} = P_{atm}$ can no longer be satisfied. Instead of $P_{wh} = P_{atm}$ (*Eq. 17*), the choked-flow condition, $c_{wh} - u_{wh} = 0$, must be used:

$$rT_c + \left(\frac{\gamma-1}{2\gamma}\right)\dot{\mu}^2 v_c^2 - \left(\frac{\gamma+1}{2\gamma}\right)\dot{\mu}^2 v_{wh}^2 = 0 \tag{20}$$

Eliminating $\dot{\mu}^2$ between (16) and (20) leads to:

$$\left(v_{wh}^2/v_c^2\right) - 1 - Log\left(v_{wh}^2/v_c^2\right) = [4\gamma/(\gamma+1)]FH$$

which proves that v_{wh}/v_c is a function of γ and FH and that:

$$\dot{\mu}v_c = I(\gamma, FH)\sqrt{rT_c}$$

Combining again with Equation (8) leads to:

$$\dot{v}_c = \Sigma\sqrt{rT_c}I(\gamma, FH)/V_0 \tag{21}$$

Equations (18) or (21), together with Equation (6), allow computation of gas temperature and specific-volume evolutions of gas during a blowout.

4 THE MOSS BLUFF BLOWOUT

In August 2004, Cavern #1 of the Moss Bluff natural gas storage in Texas experienced a major gas release and fire (*Fig. 2*). The cavern bottom was filled with saturated brine, and the volume of the gas-filled part of the cavern was V_0 = 1 268 000 m^3. The blowout initiated during de-brining of the cavern when gas entered the 8-⅝" brine string, causing the pipe to burst at ground level. The ensuing fire resulted, 21 hours (0.88 day) later, in

Figure 2

Moss Bluff blowout. From a) Rittenhour and Heath (2012); b) Cavern#1 profile, from Brouard Consulting and RESPEC (2013).

separation of the wellhead assembly and the uncontrolled loss of gas from the 20" production casing. The fire self-extinguished about 6-½ days later, when all the gas was burned off. More than 6 sbcf of gas had been released.

Several witnesses report that, after the natural-gas release had been completed, air at ground level was "sucked" into the cavern over several dozens of minutes. One possible explanation is that, during the blowout, the cavern gas was oversaturated with water vapor: partial pressure of the vapor dropped, but not enough time was left for the vapor to condense fully and to reach thermodynamic equilibrium with the brine sump at the bottom of the cavern. When the blowout was complete, additional condensation took place, leading to a decrease in the cavern gas pressure, and air was sucked into the cavern.

The surface of the cavern walls (not including the brine-gas interface) was computed to be $\Sigma_c = 84\ 200\ \text{m}^2$. The friction factor was assumed to be $f = 0.012$ when diameter is $D = 8\text{-}\frac{5}{8}$ inches and $f = 0.010$ when the well diameter is $D = 20$ inches. The borehole length is $H = 765$ m. The gas initial pressure and temperature were assumed to be $P_c^0 = 13.89$ MPa and $T_c^0 = 51°\text{C}$ (324.15 K).

Main results are presented in Figure 3. It was said that after 21 hours (0.88 day), the well diameter increased from $D = 8\text{-}5/8$" to $D = 20$". As a result of this diameter increase, head losses are smaller and gas velocities are faster; the rate of pressure and temperature changes, and the heat flux from the rock mass abruply increases. Total duration of the computed flow is slighly less than 6 days (the actual duration was 6.5 days). Gas flow is choked (gas velocity is sonic at the wellhead) during the first 3.5 days. Later, the cavern gas pressure becomes much smaller, resulting in slower velocities and normal flow.

Gas temperature in the cavern drops to $T_c = -5°\text{C}$ in two days before slowly warming. At this point, gas temperature at the wellhead is $T_{wh} = -40°\text{C}$. Cavern temperature reaches a minimum when the energy change rate generated by gas expansion exactly balances the heat-flux rate from the rock mass, as predicted by Equation (6). At the blowout climax, heat flux from the rock mass is approximately 50 MW.

The "end" of the blowout is a difficult notion to define. It can be seen in Figure 3, however, that, during day 5, the gas-flow velocity rapidly decreases and is almost nill after 5.8 days. However, thermal equilibrium between cavern gas and rock mass is not reached, and the cavern gas slowly warms, resulting in a gas outflow of approximately $u_c \simeq u_{wh} \approx 1$ m/s; the pressure difference between the cavern and ground level is no longer the driving force for gas flow. As was mentioned before, the actual validity of the mathematical solution at the end of the blowout is arguable, as water vapor condensation, for instance, may play a significant role. Note also that, at the end of the blowout, gas temperature increase is fast: gas density is small (pressure is atmospheric) and gas volumetric heat capacity is much smaller than it was before the blowout. For this reason, as explained in Section 1.3, significant temperature changes are not

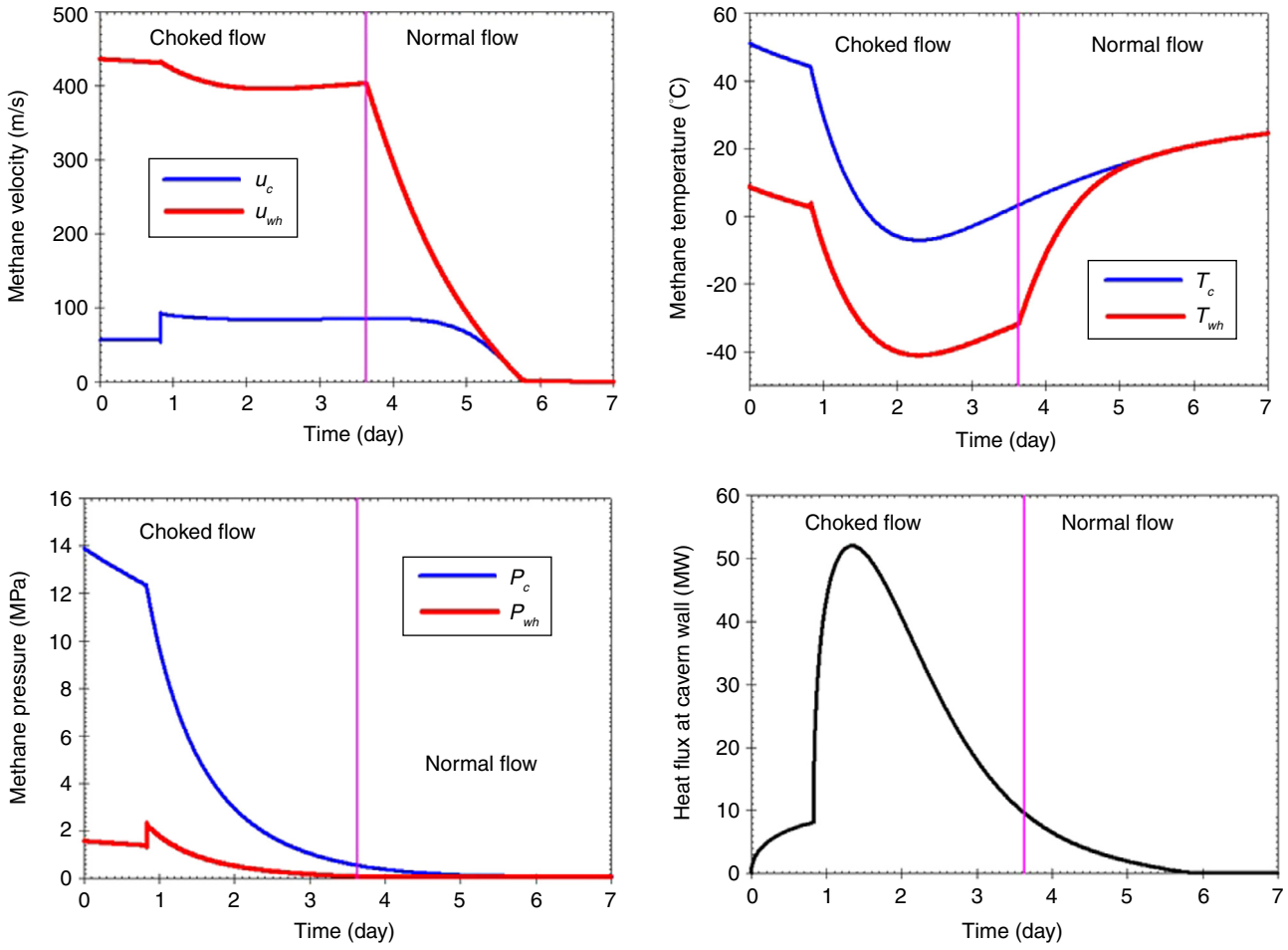

Figure 3

Computed evolutions of gas velocity, gas temperature, gas pressure and heat flux from the cavern wall as a function of time during the Moss Bluff blowout.

given time enough to penetrate deep into the rock mass. Significant tensile stresses are observed in a thin "skin" at cavern wall and deep fractures cannot develop (Brouard Consulting and RESPEC, 2013).

5 THE KANOPOLIS BLOWOUT

Compressed Air Energy Storage (CAES) is experiencing a rise in interest, as it can be used as buffer energy storage in support of intermittent sources of renewable energy, such as wind mills. We discuss here an air blowout that occurred in an abandoned mine that presents some similarities with the case of a blowout in an air storage cavern and provide some validation of the model. Obviously, in sharp contrast with natural gas or hydrogen, air cannot burn or explode, and less severe consequences must be expected from an air blowout.

Van Sambeek (2009) gave a complete account of a remarkable accident in an abandoned salt mine, and provided a comprehensive and convincing explanation of that event. "*On October 26, 2000, a brick factory in Kanopolis, Kansas, was substantially destroyed by bricks, sand, and water falling from the sky. The jet of air blew from a previously sealed salt mine shaft and through a pile of bricks next to the brick factory*" (p. 620; *Fig. 4*). Bricks and sand were blown into the air more than 100 m "*for longer than 5 minutes but less than 20 minutes*" (p. 621). The hypothesis analyzed by Van Sambeek was that "*groundwater had entered the mine through the shafts over a long time and compressed the air within the mine*" until the shaft plug collapsed in October 2000 and air escaped from the mine.

Figure 4
Kanopolis brick factory after the blowout (Van Sambeek, 2009).

The Kanopolis Mine is not a salt cavern and, in the context of a blowout, several differences are noted. The cross-sectional area of the access well (a mine shaft) is larger than the cross-sectional area of a cavern borehole by two orders of magnitude, making blowout duration much shorter (10 or so minutes instead of several days).

The shaft, lined with wood timber, had a length of $H = 240$ m, and its inside dimensions were about 3.6 m × 5.2 m. An equivalent circular cross-section, $S = 18.72$ m^2, and a friction coefficient, $F = 0.225/\text{m}$, were selected, (this value was selected to match observed data, as Colebrook's equation hardly applies to gas flow in an old wood-lined mine shaft). For air, $\gamma = 1.4$. Van Sambeek (2009) suggests that the compressed-air (absolute) pressure might have been $P_c^0 = 0.272$ MPa (0.172 MPa relative) and that the air volume in the mine was $V_0 = 670\ 000$ m^3. We assume that the initial air temperature was $T_c^0 = 15$°C (288 K).

It might have been expected that the drop in the mine's air temperature would be much more severe than in a conventional gas-storage cavern, as heat provided by the rock mass seems not to be given enough time to warm the air in the mine. In fact, heat was provided by the mine roof and by the dry surface of the pillars, whose overall surface is approximately $\Sigma_c = 1\ 000\ 000$ m^2. (No attempt was made to take into account the heat transferred from the brine that filled the lower part of the mine rooms.) The ratio between the wall area and the mine volume in Equation (9) (or $\Sigma_c/V_0 = 1.3$ m) is much larger in a mine than it is in a cavern, making the heat flux from the rock mass much faster.

Results are provided in Figure 5. The flow is normal (not choked). At ground level, air speed decreases from 180 m/s (650 km/h) to a few m/s in 11 minutes. This result is consistent with what was reported by Van Sambeek (2009) who proved that an air-stream speed of 180 m/s generates a drag force that is able to propel bricks perhaps as high as 100 m (*Fig. 6*). Figure 5 also displays air pressure and temperature during the blowout. Air temperature at ground level drops first to 1°C before increasing to 14°C at the end of the blowout. Air temperature in the mine does not experience changes larger than 1°C. Note (*Fig. 5*) that the heat flux from the rock mass reaches 330 MW after a few dozens of seconds.

6 HYDROGEN BLOWOUT

Salt caverns storing hydrogen (which have gas pressure in the 7-21 MPa range) are operated in the UK (Teesside,

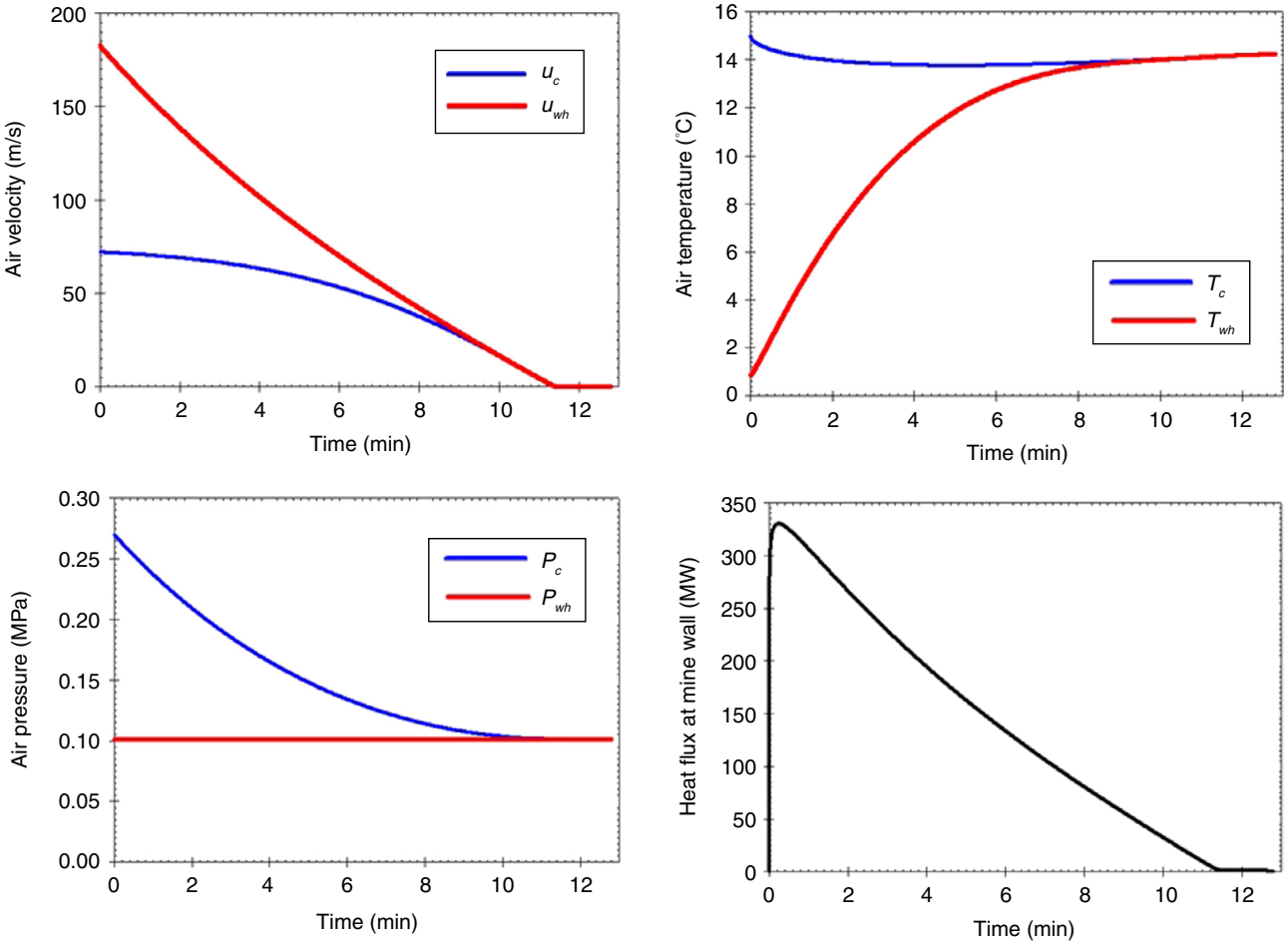

Figure 5

Computed evolution of air velocity, air temperature, air pressure and heat flux from cavern wall as a function of time during the Kanopolis blowout.

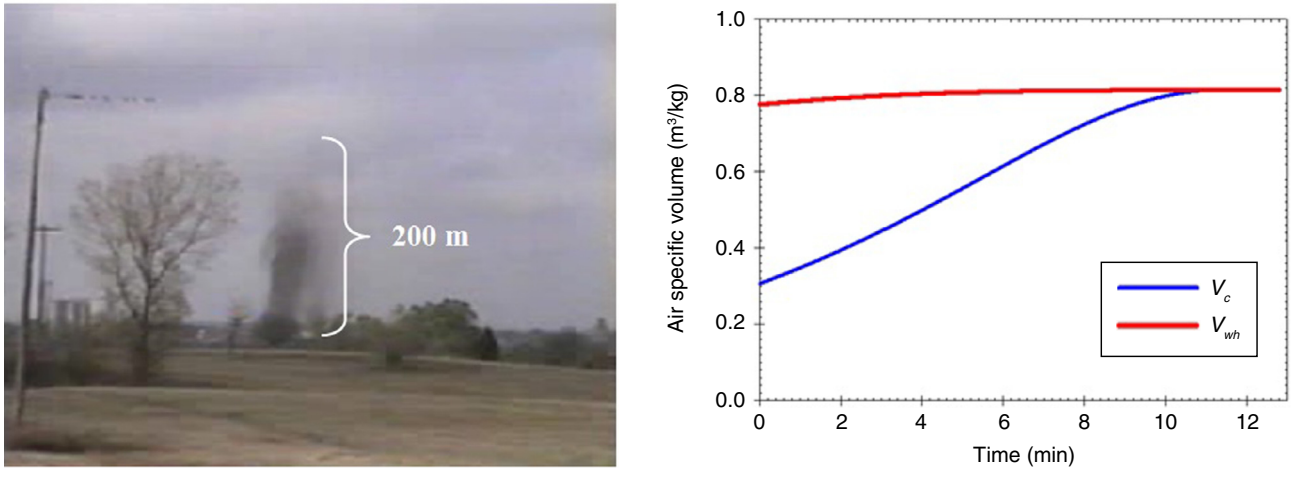

Figure 6

a) Air outflow during the blowout, videotaped from a distance of 2.5 km (Van Sambeek, 2009); b) calculated evolution of the specific volume of air as a function of time.

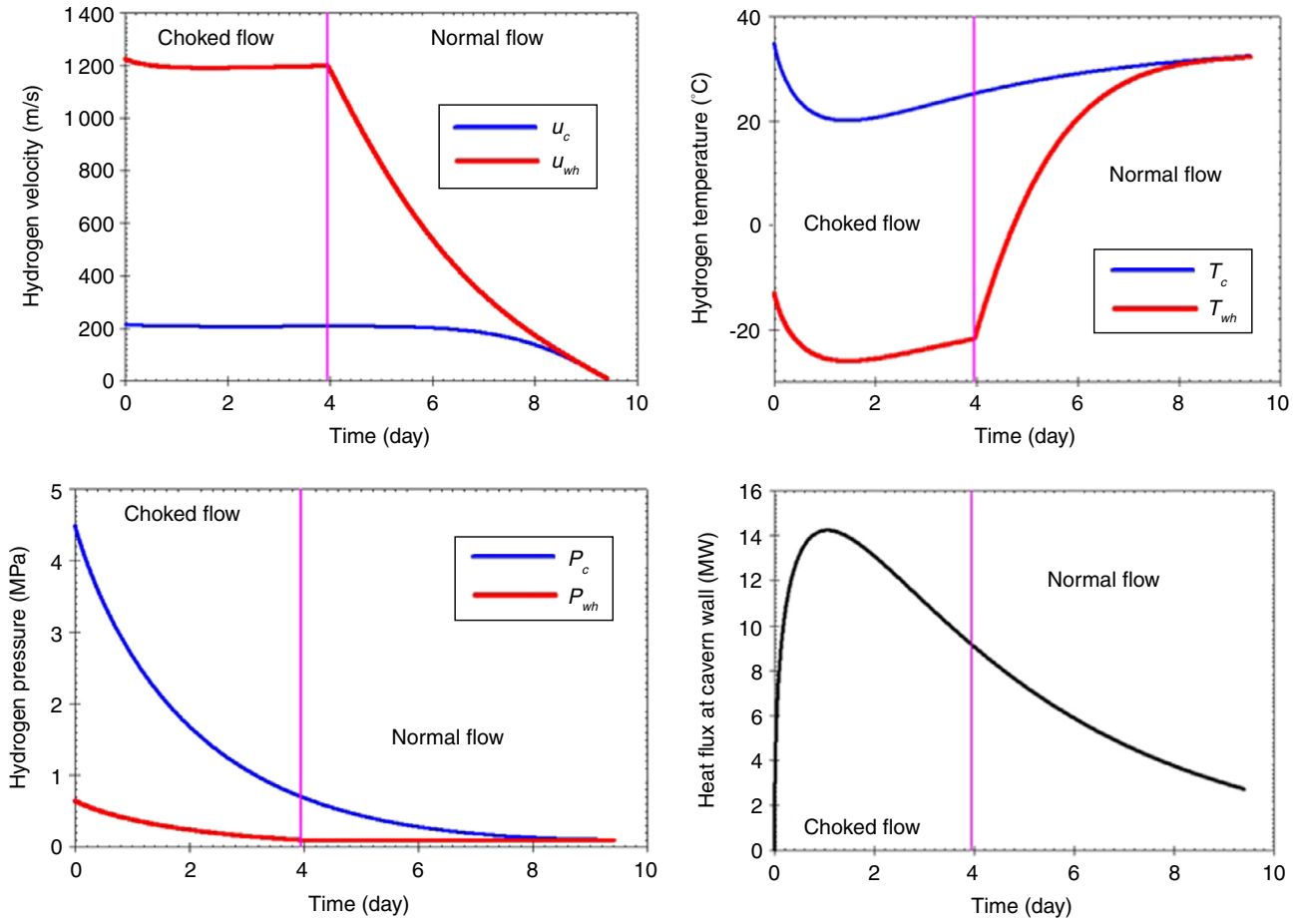

Figure 7

Computed evolution of hydrogen velocity, hydrogen temperature, hydrogen pressure and heat flux from the cavern as a function of time during a blowout.

three 70 000-m^3 caverns at a 370-m depth) and in Texas (Clemens Dome, Mont Belvieu, Moss Bluff). Hydrogen storage raises interesting problems, as its state equation and thermo-dynamic potentials differ significantly from those of an ideal gas.

6.1 Blowout from a Generic Hydrogen Storage

A discussion of a blowout from a generic hydrogen storage cavern is provided here. In this discussion, the cavern is cylindrical, with a volume $V_0 = 1\,000\,000$ m^3, an overall surface $\Sigma_c = 60\,000$ m^2, a casing-shoe depth $H = 370$ m, and tubing diameter $D = 7$". A friction factor $f = 0.01$ was selected, and the initial cavern pressure and temperature were $P_c^0 = 4.5$ MPa and $T_c^0 = 35\,^\circ$C, respectively. The thermodynamic behavior of hydrogen exhibits some specific features of interest (in particular, an isenthalpic depressurization leads to hydrogen warming); so, instead of the standard state equation of an ideal gas, a van der Waals state equation was selected to describe the gas behavior (*Appendix B*).

Main results are provided in Figure 7. The blowout is approximately 9 days long. The flow is choked during the first 4 days and is normal during the second half of the blowout. Gas velocities are high, as the speed of sound in hydrogen ($c \approx 1200$ m/s) is much faster than in air or natural gas ($c^2 \approx \gamma r T, r = C_p - C_v$, and hydrogen heat capacities are large; *Tab. 1*). The same argument (large heat capacity) explains why the temperature drop in the cavern (the temperature plummets to 20°C) is not very large (*Eq. 13*). However, the temperature drop in the

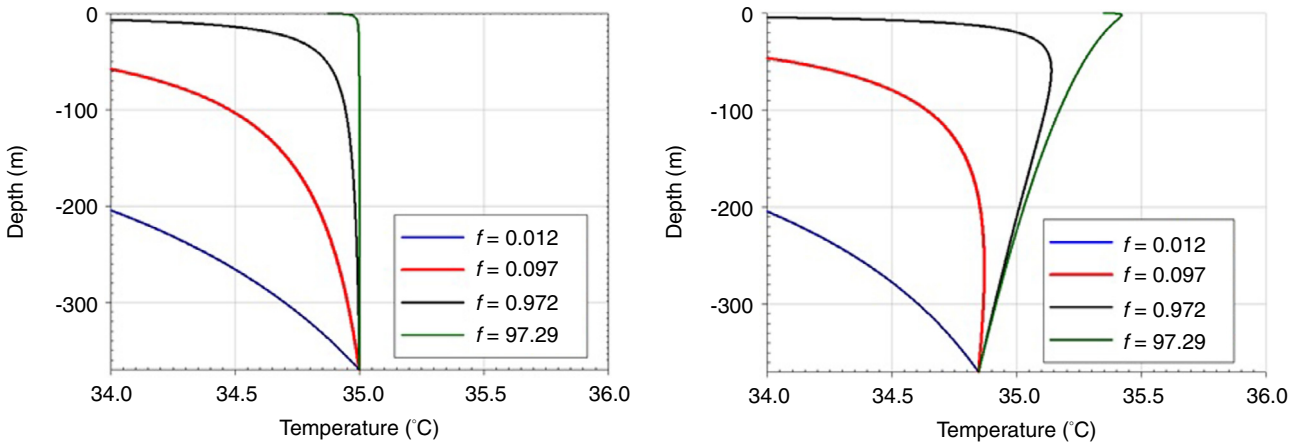

Figure 8

Temperature distribution in the well: when head losses are extremely large, hydrogen temperature increases in the well a), an effect that is not captured when the state equation of gas is ideal b).

well is not very different from what it is during a natural gas blowout, as the value:

$$T_c - T_{wh} = \left[u^2/2C_p\right]_c^{wh} \approx \gamma r T_c/2C_p \approx (\gamma - 1)T_c/2\gamma$$

is not very different from one gas to another. No hydrogen warming in the well was observed.

The same computations were performed when assuming that hydrogen is an ideal gas (instead of a van der Waals gas). Only tiny differences were observed; however, this conclusion may be wrong in some cases, as explained in the next section.

6.2 Joule-Thomson Effect

It can be observed in Figure 7 that, except at the end of the blowout, the wellhead temperature (T_{wh}) is much colder than the cavern temperature (T_c): the temperature of hydrogen decreases when it travels from the cavern top to the ground surface. However, it is known that when a real gas (as differentiated from an ideal gas) expands through a throttling device (the so-called Joule-Thomson expansion), its enthalpy remains constant, and gas temperature may either decrease or increase. Gases have a Joule-Thomson inversion temperature above which the gas temperature increases during an isenthalpic expansion. For hydrogen, this inversion temperature is −71°C (much lower than the temperatures considered here).

However, the expansion of a gas during a blowout is not a Joule-Thomson expansion, as kinetic energy cannot be neglected (*Eq. 9*). It is expected that hydrogen temperature increases during its expansion when kinetic energy can be neglected — *i.e.*, when head losses are large.

An example of a hydrogen blowout involving gas-temperature increase is presented in Figure 8. Parameters are the same as presented in Section 6.1 except for the friction factor, which is $f = 97.3$ instead of $f = 0.01$. (Head losses are larger by a factor of 10 000.) The celerity of gas flow in the well is much smaller (it is divided by a factor of 10) than in the example described in Section 6.1, and the cavern is emptied in one year or so ("blowout" is somewhat of a misnomer). The hydrogen temperature is slightly warmer at ground level than it is in the cavern, an effect that is not captured when the state equation of gas is ideal. It can be concluded that, when realistic blowout scenarios are considered, the Joule-Thomson effect plays a minor role.

CONCLUSIONS

A simplified solution was proposed to compute the evolution of gas pressures, temperatures and velocities during a blowout in a gas storage cavern. It was shown that, in general, the flow is choked when gas pressure in the cavern is high and is normal when the cavern pressure is low. Results must be considered as indicative rather than exact, as simple gas state equations and thermodynamic potentials were selected. Validation of the model is difficult: for obvious practical reasons, few parameters can be measured accurately during a

blowout. However, the thermodynamic model of the cavern is able to explain correctly the evolution of cavern gas temperature during a (controlled) gas withdrawal; duration of the Moss Bluff blowout can be back-calculated correctly; and the computed air velocities are compatible with the ballistic flight of bricks observed during the Kanopolis blowout, as was proved by Van Sambeek (2009). It is believed that this model provides a good basis for computation of the thermomechanical behavior of cavern walls during a blowout, a concern of special significance for two reasons: it is important, before a blowout, to establish a credible scenario (gas rate, duration) and, after a blowout, to assess if the caverns can be operated again.

ACKNOWLEDGMENTS

The authors thank Ron Benefield and his colleagues from Spectra Energy Transmission, and the Solution Mining Research Institute (SMRI), which granted permission that some results of the Moss Bluff Cavern#1 analysis performed for the SMRI (Research Report 2013-01) be published in this paper. They also are indebted to Leo van Sambeek, who provided them with additional comments on his remarkable analysis of the Kanopolis accident. Special thanks to Kathy Sikora. This study was funded partially by the French *Agence Nationale de la Recherche* (ANR) in the framework of the SACRE Project devoted to adiabatic CAES design. This project includes researchers from EDF, GEOSTOCK, PROMES (Perpignan), HEI (Lille) and École Polytechnique ParisTech (Palaiseau).

REFERENCES

Air liquide (2012) *Gas Encyclopedia*, < http://encyclopedia.airliquide.com > .

Alberta Energy and Utilities Board (2002) *BP* Canada Energy Company: Ethane Cavern well fires, Fort Saskatchewan, Alberta, Aug./Sept. 2001, *EUB post incident report*.

Bérest P., Brouard B. (2003) Safety of salt caverns used for underground storage, *Oil & Gas Science and Technology – Rev. IFP* **58**, 3, 361-384.

Bérest P., Djizanne H., Brouard B., Hévin G. (2012) Rapid Depressurizations: can they lead to irreversible damage? *Proc. SMRI Spring Technical Conference*, Regina, Canada, 24-23 April, 63-86.

Bérest P., Djizanne H., Brouard B., Frangi A. (2013) A Simplified Solution For Gas Flow During a Blow-out in an H_2 or Air Storage Cavern, *Proc. SMRI Spring Technical Conference*, Lafayette, Louisiana, 23-23 April, 86-94.

Brouard Consulting and RESPEC (2013) Analysis of Cavern MB#1 Moss Bluff Blowout data, *Research Report 2013-01*, *Solution Mining Research Institute*, 197 pages.

Crotogino F., Mohmeyer K.U., Scharf R. (2001) Huntorf CAES: More than 20 Years of Successful Operation, *Proc. SMRI Spring Technical Conference*, Orlando, Florida,15-18 April, 351-362.

Crossley N.G. (1996) Salt cavern Integrity Evaluation Using Downhole Probes. A Transgas Perspective, *Proc. SMRI Fall Meeting*, Cleveland, Ohio, 21-54.

Krieter M. (2011) Influence of gas cavern's surface area on thermodynamic behavior and operation, *Proc. SMRI Fall Technical Conference*, York, UK, 179-184.

Landau L., Lifchitz E. (1971) *Mécanique des Fluides*. Éditions MIR. (in French).

Ma L., Liu X., Xu H., Yang S., Wang Z. (2011) Stability analysis of salt rock gas storage cavern under uncontrolled blowout, *Rock and Soil Mechanics* **32**, 9, 2791-2798 (in Chinese).

Rittenhour T.P., Heath S.A. (2012) Moss Bluff Cavern 1 Blowout, *Proc. SMRI Fall Technical Conference*, Bremen, Germany, 119-130.

Van Sambeek L. (2009) Natural compressed air storage: a catastrophe at a Kansas salt mine, *Proc. 9th Int. Symp. on Salt*, Beijing, Zuoliang Sha ed., Vol. 1, 621-632.

Von Vogel P., Marx C. (1985) Berechnung von Blowoutraten in Erdgassonden, *Erdoel-Erdgas*, 101.Jg, Heft 10, Oktober 1985, 311-316 (in German).

Manuscript accepted in November 2013
Published online in May 2014

Appendix A – Gravity Forces

From Equations (9) and (10) in the main text, it is seen that gravity forces may play a significant role when gH is not much smaller than $[u^2/2]_c^{wh}$. Because gH typically is 10 000 m^2/s^2, gravity forces must be taken into account when $u_{wh} \approx 100$ m/s — *i.e.*, when the flow is normal. When gravity forces are taken into account ($g \neq 0$),the following equations apply (instead of Eq. 13, 14 and 15).

$$C_P T + \dot{\mu}^2 v^2/2 + gz = C_P T_c + \dot{\mu}^2 v_c^2/2 \tag{A1}$$

$$P = \left(P_c + \frac{\gamma-1}{2\gamma}\dot{\mu}^2 v_c\right)\frac{v_c}{v} - \frac{\gamma-1}{2\gamma}\left(\dot{\mu}^2 v + \frac{2gz}{v}\right) \tag{A2}$$

$$\left(rT_c + \frac{\gamma-1}{2\gamma}\dot{\mu}^2 v_c^2\right)\frac{1}{v} - \frac{\gamma+1}{2\gamma}\dot{\mu}^2 v - \frac{\gamma-1}{\gamma}\frac{gz}{v} = \left(\frac{g}{\gamma} + F\dot{\mu}^2 v^2\right)\frac{dz}{dv} \tag{A3}$$

The solution of the differential equation (A3) can be written as:

$$F\dot{\mu}^2 H = v_{wh}^{1-\gamma}\left(\frac{g}{\gamma F\dot{\mu}^2} + v_{wh}^2\right)^{\frac{\gamma-1}{2}} \int_{v_c}^{v_{wh}} \frac{\left(rT_c + \frac{\gamma-1}{2\gamma}\dot{\mu}^2 v_c^2\right)\frac{1}{w} - \frac{\gamma+1}{2\gamma}\dot{\mu}^2 w}{w^{1-\gamma}\left(\frac{g}{\gamma F\dot{\mu}^2} + w^2\right)^{\frac{\gamma+1}{2}}} dw \tag{A4}$$

$$P_{wh} = \left(rT_c + \frac{\gamma-1}{2\gamma}\dot{\mu}^2 v_c^2\right)\frac{1}{v_{wh}} - \frac{\gamma-1}{2\gamma}\left(\dot{\mu}^2 v_{wh} + \frac{2gH}{v_{wh}}\right) \tag{A5}$$

Equations (A4) and (A5) allow to compute v_{wh}, $\dot{\mu}^2$ etc. Main results are provided in Figure A1 ($g = 10$ m/s^2), which must be compared to the corresponding results provided in Figure 5 ($g = 0$ m/s^2) in the main text. Differences are

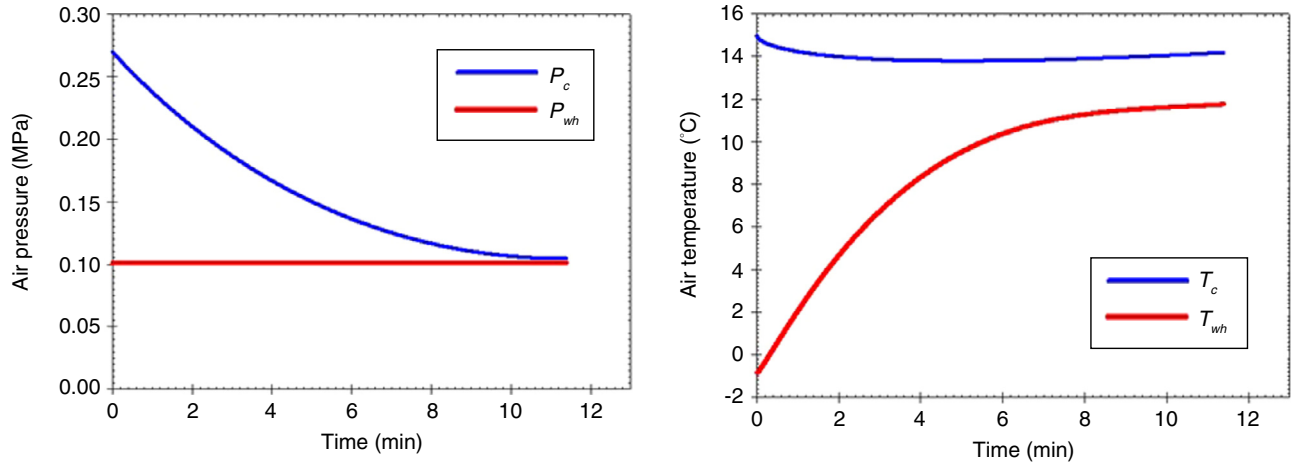

Figure A1

Kanopolis blowout ($g = 10$ m/s^2): computed evolutions of a) air pressure and b) air temperature as a function of time.

exceedingly small, except at the end of the blowout, as static pressure and temperature distributions in the well are modified by gravity forces. Equations (A1) and (A2) prove that, when thermodynamic equilibrium is reached, $T_{wh} = T_\infty - (gH/C_p) = 12.6°C$ (instead of: $T_{wh} = T_\infty = 15°C$) and that $P_c = P_{wh}(T_\infty/T_{wh})^{\frac{\gamma}{\gamma-1}} = 1.003\ P_{wh}$ (instead of: $P_c = P_{wh} = P_{atm}$). This solution is partly artificial, as it results from various assumptions that are not fully consistent. (Well walls are adiabatic; cavern walls are not.)

Appendix B – Hydrogen Flow

It is known that hydrogen exhibits special behavioral characteristics — in particular, during depressurization such that hydrogen enthalpy is constant (for instance, when hydrogen leaks from a pressurized vessel through a pinhole), the temperature of hydrogen "increases". (For most gases in similar circumstances, the temperature decreases). For this reason, instead of the ideal gas equation, the more precise van der Waals equation is used:

$$P = -\frac{a}{v^2} + \frac{rT}{v-b} \tag{B1}$$

where a and b are constants. It can be assumed that the temperature is above the critical temperature, $T_{cr} = 33.2$ K (which means that (B1) allows computation of v when P and T are known). The internal energy and enthalpy of hydrogen are:

$$\begin{cases} e(T,v) = C_v T - \frac{a}{v} \\ h(T,v) = e + Pv = C_v T - \frac{2a}{v} + \frac{rTv}{v-b} \end{cases} \tag{B2}$$

The same method as used for air can be used here: energy equation allows computation of pressure and temperature. Let $\bar{C}_p = C_v + r$ (for a van der Waals gas, $\bar{C}_p$ is not the heat capacity at constant pressure, C_p) and $\bar{\gamma} = \bar{C}_p/C_v$:

$$T = (\bar{\gamma}-1)(v-b)\frac{h_c + \frac{1}{2}\dot{\mu}^2 v_c^2 + \frac{2a}{v} - \frac{1}{2}\dot{\mu}^2 v^2}{r(v\bar{\gamma}-b)} \tag{B3}$$

$$P = -\frac{a}{v^2} + (\bar{\gamma}-1)\frac{h_c + \frac{1}{2}\dot{\mu}^2 v_c^2 + \frac{2a}{v} - \frac{1}{2}\dot{\mu}^2 v^2}{\bar{\gamma}v-b} \tag{B4}$$

When one sets:

$$\psi(v,\dot{\mu}) = \frac{\bar{\gamma}}{b^2}\left(h_c + \frac{1}{2}\dot{\mu}^2 v_c^2 + \frac{2a\bar{\gamma}}{b}\right)\left(\frac{b}{(\bar{\gamma}v-b)} + Log\left(\frac{v\bar{\gamma}-b}{v}\right)\right)$$

it can be inferred that:

$$\left[-\frac{2a}{3v^3} + (\bar{\gamma}-1)\left[-\frac{a}{bv^2} + \psi(v,\dot{\mu}) - \frac{1}{2\bar{\gamma}}\dot{\mu}^2 Log(v\bar{\gamma}-b) - \frac{\dot{\mu}^2 v}{2(\bar{\gamma}v-b)}\right]\right] + \dot{\mu}^2 Log(v) = -F\dot{\mu}^2\frac{dz}{dv} \tag{B5}$$

Instead of Equations (16, 17) and (19) when $g = 0$, we now have:

$$\left[-\frac{2a}{3v^3} + (\bar{\gamma}-1)\left[-\frac{a}{bv^2} + \psi(v,\dot{\mu}) - \frac{1}{2\bar{\gamma}}\dot{\mu}^2 Log(v\bar{\gamma}-b) - \frac{\dot{\mu}^2 v}{2(\bar{\gamma}v-b)}\right] + \dot{\mu}^2 Log(v) = -FH\dot{\mu}^2\right]_{v_c}^{v_{wh}} \tag{B6}$$

$$P_{wh} = -\frac{a}{v_{wh}^2} + (\bar{\gamma}-1)\frac{h_c + \frac{1}{2}\dot{\mu}^2 v_c^2 + \frac{2a}{v_{wh}} - \frac{1}{2}\dot{\mu}^2 v_{wh}^2}{\bar{\gamma}v_{wh}-b} \tag{B7}$$

$$c^2 - u^2 = -\frac{2a}{v} + \frac{v^2}{(v-b)}\bar{\gamma}(\bar{\gamma}-1)\frac{h_c + \frac{1}{2}\dot{\mu}^2 v_c^2 + \frac{2a}{v} - \frac{1}{2}\dot{\mu}^2 v^2}{v\bar{\gamma} - b} - \dot{\mu}^2 v^2 > 0 \tag{B8}$$

Here, again, when inequality (B8) is met (normal flow), Equations (B6) and (B7) allow elimination of $\dot{\mu}^2$ and computation of v_{wh}. When inequality (B8) is not met (choked flow), Equation (B6) together with the condition $c_{wh}^2 - u_{wh}^2 = 0$, as given in (B9):

$$-\frac{2a}{v_{wh}^3} + \frac{\bar{\gamma}(\bar{\gamma}-1)\left(h_c + \frac{2a}{v_{wh}}\right)}{(v_{wh}-b)(v_{wh}\bar{\gamma}-b)} = \dot{\mu}^2\left[1 + \frac{\bar{\gamma}(\bar{\gamma}-1)\left(v_{wh}^2 - v_c^2\right)}{2(v_{wh}-b)(v_{wh}\bar{\gamma}-b)}\right] \tag{B9}$$

allow for computation of v_{wh} This is shown in Figure B1.

An example is provided here. Hydrogen properties are provided in Table 1 in the main text. In Figure B1a, cavern temperature and pressure are $T_c = 313.15$ K and $P_c = 0.5$ MPa, respectively, resulting in an inlet hydrogen specific volume $v_c = 2.6$ m^3/kg. The well is 1000-m deep, the well diameter is 0.5 m and the friction factor is $f = 0.01$. Equations (B6, B7) and (B9) allow three curves to be drawn: $\dot{\mu}_{FH}^2 = \dot{\mu}_{FH}^2(v_{wh})$, $\dot{\mu}_{atm}^2 = \dot{\mu}_{atm}^2(v_{wh})$ and $\dot{\mu}_{son}^2 = \dot{\mu}_{son}^2(v_{wh})$, respectively. The grey zone is the supersonic zone, in which $c_{wh} < u_{wh}$ (not acceptable). The intersection of the curves described by Equations (B6) and (B7), obtained when the specific volume at the exit is $v_{wh} = 11.4$ m^3/kg, can be accepted, as it lays outside the supersonic zone: the flow is normal.

In Figure B1b, cavern temperature and pressure are $T_c = 313.15$ K and $P_c = 13$ MPa, respectively, resulting in an inlet gas specific volume $v_c = 0.10$ m^3/kg. Here, again, $FH = 10$. The intersection of the curves representing (B6) and (B7) belongs to the gray supersonic zone and does not provide an acceptable solution: the flow cannot be normal. The flow is choked, and the specific volume at the exit, $v_{wh} = 0.55$ m^3/kg, is given by the intersection of the curves described by (B6) and (B9): $\dot{\mu}_{FH}^2 = \dot{\mu}_{FH}^2(v_{wh})$ and $\dot{\mu}_{son}^2 = \dot{\mu}_{son}^2(v_{wh})$. Note that, at this intersection, the curve $\dot{\mu}_{FH}^2 = \dot{\mu}_{FH}^2(v_{wh})$ reaches a maximum, as $v_{wh} - c_{wh} = 0$.

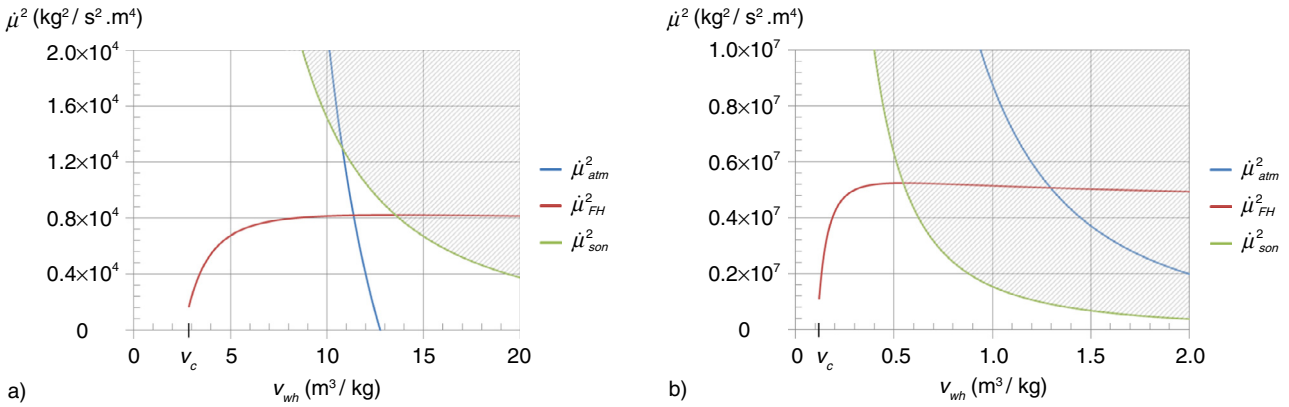

Figure B1

Determination of the specific volume of hydrogen at the exit, v_{wh}, in the case of a) normal flow and b) choked flow.